H-bond patterns and structure distributions of water octamer $(H_2O)_8$ at finite temperatures

Toshiko Miyake, Misako Aida*

Center for Quantum Life Sciences and Department of Chemistry, Graduate School of Science, Hiroshima University, Kagamiyama, Higashi-Hiroshima, 739-8526 Japan

Abstract

The NVT ensemble of water octamer is divided into the configurational subsets, which correspond to the topology-distinct H-bond patterns, and the relative molar Helmholtz energies of the H-bond patterns are evaluated. The method is based on the combination of standard Monte Carlo techniques with defined H-bond patterns. The structure distributions of water octamers at 200 and 300 K are presented based on the H-bond patterns instead of the 'inherent structures'. The thermodynamically favored structures of water octamer, which are energetically favored and readily feasible (entropy-favored for cluster formation), are presented.

* Corresponding author. FAX: +81-82-424-0725
  e-mail address: maida@hiroshima-u.ac.jp (Misako Aida).

1. Introduction

A hydrogen-bond (H-bond) network is formed in a water cluster [1-9]. Extensive attention has been directed to locating all the local minimum structures on the potential energy surface (PES) of water clusters [9,10] and finding the global minimum structure for each system [6-8,11].

A water cluster is relevant to a digraph and can be classified to an H-bond pattern [2,3,12]. We have shown that the numbers of topology-distinct H-bond patterns of $(H_2O)_n$ are 5, 22, 161, 1406, 14241 and 164461 for n=3-8, respectively, using the H-bond matrix by graph-theoretical enumeration. A water cluster at finite temperature has a structure that corresponds to one of these topologically distinct H-bond patterns.

Water octamer, $(H_2O)_8$, has been the subject of considerable theoretical studies [5-7, 11-28 and references therein]. Several local minimum structures are located on the PES by means of the Monte Carlo (MC) simulated annealing procedure or the jump-walking method [4,13]. Two nearly isoenergetic and most stable structures [6,11,13,14,18-21] are shown in Fig. 1, as **12A** (D_{2d}) and **12B** (S_4) together with their H-bond patterns, where twelve H-bonds form the cubic H-bond network.

In the present letter, we show a new concept to divide the configurational space according to the H-bond patterns and present thermodynamically favored structures of water octamer, which are *not* based on the 'inherent structures' *but* the H-bond patterns.

2. Methods

2.1. H-bond pattern and digraph

An H-bond pattern in water cluster can be represented by digraph, and it corresponds to the H-bond matrix [2]. A digraph has a set of information on the H-bond

connectivity between any two of the constituent water molecules. Here we describe the H-bond patterns in a decomposed water cluster system using non-connected digraphs. There are 164461 topology-distinct connected H-bond patterns corresponding to water octamer; 183120 H-bond patterns, including decomposed cluster.

2.2. Monte Carlo sampling

We coded our own program to create the configurations of water clusters so as to form the NVT ensemble (at constant number N, volume V and temperature T) using the MC method based on the Metropolis algorithm [29] and to analyze the water cluster distribution by means of the H-bond matrix [2]. We adopt the periodic boundary condition to keep the volume of the system constant with a constant number of the constituent water molecules; i.e., the density of the water cluster is defined. The two-body interactions are restricted to those between eight water molecules which are nearest neighbors in the periodic image, and the total number of the interactions is kept constant in the MC simulations.   In this procedure, we set the simulation box to be so large that we can regard the system as being composed of an isolated cluster.   The size of the box is set to be 51.0 Å, which corresponds to 80 L for 1 mol of water cluster.

A set of TIP3P potential functions was used for the energy calculation [30], which is represented by the sum of two-body interactions.   Starting from several initial geometries which were sufficiently distinct, the following procedure was taken.   First, 10^8 MC steps of equilibration were performed at 400 K.   Then the simulated annealing was repeated with 20 K decrement in temperature and 10^8 MC steps of equilibration at each temperature until the system reached the final temperature (200 or 300 K).   And

then, 10^9 MC steps at the temperature were performed and used for the analysis.

2.3. Subsets of NVT ensemble

The NVT ensemble is a set of water cluster configurations. Given a criterion of H-bond between any two of the constituent molecules, one can define an H-bond pattern for each configuration in the NVT ensemble. In the current simulation, we define the formation of H-bond when an H-bond distance (between a donor proton and an acceptor oxygen) is less than 2.45 Å [31] and an H-bond angle (O-H…O) exceeds 120°. The NVT ensemble is classified into the subsets according to the H-bond patterns.

2.4. Helmholtz free energy and internal energy of subset

The NVT ensemble of water octamer is formed by the MC simulation at temperature T with a fixed density. The Helmholtz energy A of the system is related to the partition function Q of the system,

$$A = -k_{\mathrm{B}} T \ln Q \quad .$$ (1)

The system is comprised of subsets (H-bond patterns). The following values are obtained from this MC simulation:

$$Q = \sum_I \sum_{i \in I} \exp\left(-\frac{E_i}{k_{\mathrm{B}} T}\right) = \sum_I Q_I \quad ,$$ (2)

$$N_{\mathrm{total}} = \sum_I N_I \quad ,$$ (3)

and

$$Q_I / Q = N_I / N_{\mathrm{total}} \equiv x_I \quad .$$ (4)

Here, x_I is the mole fraction of a subset I, which is equal to the ratio of the number of the configurations for subset I, N_I, to the number of configurations for the whole system,

N_{total}, of the MC simulation. For each subset I, the energy average $\langle E \rangle_I$ is obtained by

$$\langle E \rangle_I = \frac{\sum_{I \in i} E_i}{N_I} \qquad . \tag{5}$$

In the current study, we calculate the energy using the TIP3P potential function and the structure of each water molecule is fixed. The calculated energy of a water cluster corresponds to the interaction energy between 8 water molecules per 1 mol of cluster. The molar internal energy $\overline{U}_I(T)$ of subset I at temperature T is related to the energy average of subset I as

$$\overline{U}_I(T) = \overline{U}(0) + \langle E \rangle_I \qquad . \tag{6}$$

Here, $\overline{U}(0)$ is the energy of the isolated non-interacting 8 water molecules. Note that all the quantities obtained in the current study are the values relative to those of the isolated non-interacting 8 water molecules, which are assumed to be independent of any variable (temperature etc.), because the structure of a water molecule is kept fixed.

The molar Helmholtz energy of a water cluster, which has a structure of the H-bond pattern I, at temperature T and volume V, is related to the occurrence of the water cluster. The relative molar Helmholtz energy $\Delta \overline{A}_{I-J}$ of water cluster, between the H-bond patterns I and J, is given by

$$\Delta \overline{A}_{I-J}(T) = -RT \ln \frac{x_I}{x_J} = -RT \ln \frac{N_I}{N_J} \qquad . \tag{7}$$

On the other hand, the molar Helmholtz energy of the H-bond pattern I is related to the internal energy and the entropy of the system; namely,

$$\overline{A}_I(T) - \overline{A}(0) = \overline{U}_I(T) - \overline{U}(0) - T\overline{S}_I \qquad . \tag{8}$$

Here, $\overline{A}(0)$ is the free energy of the system composed of the isolated non-interacting 8

water molecules.   The entropy of the H-bond pattern I, $\overline{S}_I$, corresponds to the 'cluster formation' entropy of the H-bond pattern I from isolated water molecules.   The relative molar Helmholtz energy between the H-bond patterns I and J is

$$\Delta \overline{A}_{I-J} = \Delta \overline{U}_{I-J} - T\Delta \overline{S}_{I-J} \qquad . \qquad (9)$$

Here, $\Delta \overline{U}_{I-J}$ is the relative internal energy between the H-bond patterns I and J. This is equal to the difference between the averaged energies of the H-bond patterns I and J; namely,

$$\Delta \overline{U}_{I-J}(T) = \langle E \rangle_I - \langle E \rangle_J \qquad . \qquad (10)$$

In Eq. (9), $\Delta \overline{S}_{I-J}$ is the relative entropy of cluster formation between the H-bond patterns I and J.   Note that the intramolecular vibrational entropy of water molecule is not evaluated in the current method since each water molecule is fixed during the MC sampling.   It corresponds to the assumption that all the terms related to the intramolecular property of each water molecule are equal in all the H-bond patterns.

3. Results and discussion

3.1. Structures at 200 K

Relative molar Helmholtz energies for the H-bond patterns (at T=200 K and V=80 L for 1 mol of cluster) are shown in Fig. 2.   Each pattern is placed in a column according to the number of the constituent H-bonds.   In each of the columns, a few H-bond patterns which have lower free energies are shown with digraph representations.   The pattern 9A is the lowest in the molar Helmholtz energy at this condition, which has two fused pentagonal cycles.   Note that the molar Helmholtz energies of any cubic structures (for example, 12A or 12B) are very high.

Internal energies are shown in Fig. 3, for some selected subsets for which sufficient configurations (more than 10^4 configurations) are obtained and which have lower energy values in each column.   In our simulations, the patterns **12A** (D_{2d}) and **12B** (S_4) are the most stable in internal energies.   This is consistent with previous reports, in which TIP3P gives the D_{2d} structure as the global minimum [6, 11].

The structures and their digraph representations of the three most abundant H-bond patterns (**9A**, **9B** and **8A**) at this condition are shown in Fig. 4, together with the Helmholtz energy, internal energy and entropy terms of each H-bond pattern relative to those of **9A**.   These three patterns occupy ~37% of the whole water octamers at this condition.   The H-bond patterns **9B** and **8A** are favored from the viewpoint of entropy of cluster formation, while they are unstable from the viewpoint of internal energy compared with **9A**.   It is noteworthy that each of **9A** and **9B** is formed by adding one more H-bond to **8A**.

3.2. Structures at 300 K

The H-bond patterns that have lower molar Helmholtz energies (at T=300 K and V=80 L for 1 mol of cluster) are shown in Fig. 5.   At this condition, the observed H-bond patterns are different from those observed at 200 K, and many decomposed H-bond patterns are observed, which may correspond to evaporation.   The pattern **6A**, which has a cyclic hexamer and two isolated water molecules in it, and the pattern **5A**, which has a cyclic pentamer and three isolated water molecules in it, have the lowest molar Helmholtz energy.   Many of the observed H-bond patterns include a cyclic or linear cluster with isolated water molecules at this condition.

3.3. Water clusters with thermal energy

The relative free energies of water clusters at the local minimum structures have been evaluated with various theoretical methods. Quantum chemical thermodynamic calculations using a high level ab initio MO method [14] predicted that the D_{2d} cubic structure had the lowest free energy and dominated the potential energy and free energy hypersurfaces from 0 to 298 K. This calculation of free energy was based on the ideal gas approximation of free particles, in which the geometry optimization of water cluster was followed by an analysis of vibrational frequencies based on the harmonic approximation. This method precisely evaluated the contributions from the rotational, vibrational and electronic terms to free energy at each local minimum structure. However, one important factor missing in this method was the entropy of cluster formation for each structure.

In contrast, the MC method can evaluate the entropy of cluster formation. In most of the MC studies, however, the distributions of 'inherent structures' at each temperature have been evaluated [5,17,33 and references therein]. The conformation of a water cluster at a given temperature is represented by one of the local minima on the PES, so-called an 'inherent structure.' Those studies have shown the high population of the cubic 'inherent structures' at 200 K, with increasing population of non-cubic species at higher temperatures [5].

Our analysis has shown a different picture. From the viewpoint of the H-bond patterns, clusters take various structures that do not correspond to any local minima at finite temperature. Our analysis gives the distribution of cluster structures among the H-bond patterns, regardless of whether the corresponding local minimum structures exist. In the present work at 200 K, for instance, the internal energies of the two cubic

structures (12A and 12B) are very low, but they occupy only 0.1% of the whole NVT ensemble. Various H-bond patterns with higher internal energies have higher contributions in the ensemble at higher temperature.

The free energy derived from our analysis includes the randomness or the probability to form effective H-bond patterns, i.e., entropy of cluster formation. The value of $\Delta \overline{U}_{I-J}$ of the H-bond pattern I indicates the energetic stability relative to J, and the values of $T\Delta \overline{S}_{I-J}$ indicates the 'feasibility' to form the H-bond pattern I relative to J from the isolated water molecules. Here we compare the stability of 9A with 11A at 200 K under such a condition. The H-bond pattern 11A is energetically more stable than 9A by 2.5 kcal/mol (Fig. 3), while the probability of formation is lower in 11A than in 9A by 4.1 kcal/mol, which makes 9A thermodynamically more favorable over 11A.

The aim of the present work is to demonstrate that the classification to the H-bond pattern corresponds to the division of the configurational space of water cluster structures, where the H-bond patterns can be used to distinguish water cluster structures at finite temperatures created by a simulation technique.

References

[1] K. Liu, J.D. Cruzan, R.J. Saykally, Science 271 (1996) 929.

[2] T. Miyake, M. Aida, Chem. Phys. Lett. 363 (2002) 106.

[3] T. Miyake, M. Aida, Internet Electron. J. Mol. Des. 2 (2003) 24.

[4] K.S. Kim, M. Dupuis, G.C. Lie, E. Clementi, Chem. Phys. Lett. 131 (1986) 451.

[5] A.N. Tharrington, K.D. Jordan, J. Phys. Chem. A. 107 (2003) 7380.

[6] H. Kabrede, R. Hentschke, J. Phys. Chem. B. 107 (2003) 3914.

[7] J. Pillardy, K.A. Olszewski, L. Piela, J. Mol. Struct. 270 (1992) 277.

[8] D.J. Wales, M.P. Hodges, Chem. Phys. Lett. 286 (1998) 65.

[9] C.J. Tsai, K.D. Jordan, J. Phys. Chem. 97 (1993) 11227.

[10] D.J. Wales, M.A. Miller, T.R. Walsh, Nature 394 (1998) 758.

[11] J.A. Niesse, H.R. Mayne, J. Comput. Chem. 18 (1997) 1233.

[12] S. McDonald, L. Ojamäe, S.J. Singer, J. Phys. Chem. A. 102 (1998) 2824.

[13] C.J. Tsai, K.D. Jordan, J. Phys. Chem. 97 (1993) 5208.

[14] M.B. Day, K.N. Kirschner, G.C. Shields, Int. J. Quantum Chem. 102 (2005) 565.

[15] S.D. Belair, J.S. Francisco, Phys. Rev. A, 67 (2003) 063206.

[16] D.J. Wales, I. Ohmine, J. Chem. Phys. 98 (1993) 7257.

[17] P. Nigra, M.A. Carignano, S. Kais, J. Chem. Phys. 115 (2001) 2621.

[18] S. Maheshwary, N. Patel, N. Sathyamurthy, A.D. Kulkarni, S.R. Gadre, J. Phys. Chem. A. 105 (2001) 10525.

[19] S.S. Xantheas, E. Aprà, J. Chem. Phys. 120 (2004) 823.

[20] J.T. Su, X. Xu, W.A. Goddard III, J. Phys. Chem. A. 108 (2004) 10518.

[21] J. Kim, B.J. Mhin, S.J. Lee, K.S. Kim, Chem. Phys. Lett. 219 (1994) 243.

[22] J.O. Jensen, P.N. Krishnan, L.A. Burke, Chem. Phys. Lett. 246 (1995) 13.

[23] C.J. Tsai, K.D. Jordan, J. Chem. Phys. 99 (1993) 6957.

[24] G. Brink, L. Glasser, J. Phys. Chem. 88 (1984) 3412.

[25] D.J. Wales, I. Ohmine, J. Chem. Phys. 98 (1993) 7245.

[26] D.J. Wales, Mol. Phys. 100 (2002) 3285.

[27] F.H. Stillinger, C.W. David, J. Chem. Phys. 73 (1980) 3384.

[28] J. Sadlej, V. Buch, J.K. Kazimirski, U. Buck, J. Phys. Chem. A. 103 (1999) 4933.

[29] N. Metropolis, A.W. Rosenbluth, M.N. Rosenbluth, A.H. Teller, E. Teller, J. Chem. Phys. 21 (1953) 1087.

[30] W.L. Jorgensen, J. Am. Chem. Soc. 103 (1981) 335.

[31] E.S. Kryachko, Chem. Phys. Lett. 314 (1999) 353.

[32] B. Kirchner, J. Chem. Phys. 123 (2005) 204116.

[33] O.M. Becker, M. Karplus, J. Chem. Phys. 106 (1997) 1495.

Figure captions

Fig. 1   Structures of **12A** (D_{2d}) and **12B** (S_4) and their digraph representations.

Fig. 2   Relative molar Helmholtz energies of water octamer (at T=200 K and V=80 L for 1 mol of cluster).   Some selected H-bond patterns are shown in digraph representations with molar Helmholtz energies relative to the lowest in parentheses.   Populations are shown in percent in square brackets.
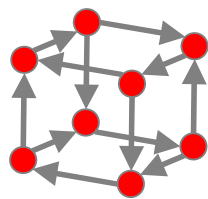
Fig. 3   Relative molar internal energy of water octamer.   Some selected H-bond patterns are shown in digraph representations with molar internal energies relative to the lowest in parentheses.

Fig. 4   Three most abundant H-bond patterns (**9A**, **9B** and **8A**) at T=200 K.   The structure shown for each H-bond pattern is a snapshot of the NVT ensemble. The relative molar Helmholtz energy $\Delta \overline{A}_I$, the relative molar internal energy $\Delta \overline{U}_I$, the relative molar entropy term $-T\Delta \overline{S}_I$ of H-bond pattern I are shown in kcal/mol.   All values are relative to those of the H-bond pattern **9A**.

Fig. 5   Relative molar Helmholtz energies for water octamer (at T=300 K and V=80 L for 1 mol of cluster).   Some selected H-bond patterns are shown in digraph representations with molar Helmholtz energies relative to the lowest in parentheses.   Populations are shown in percent in square brackets.
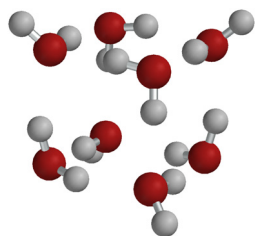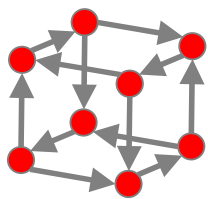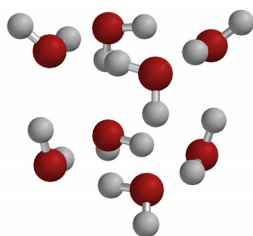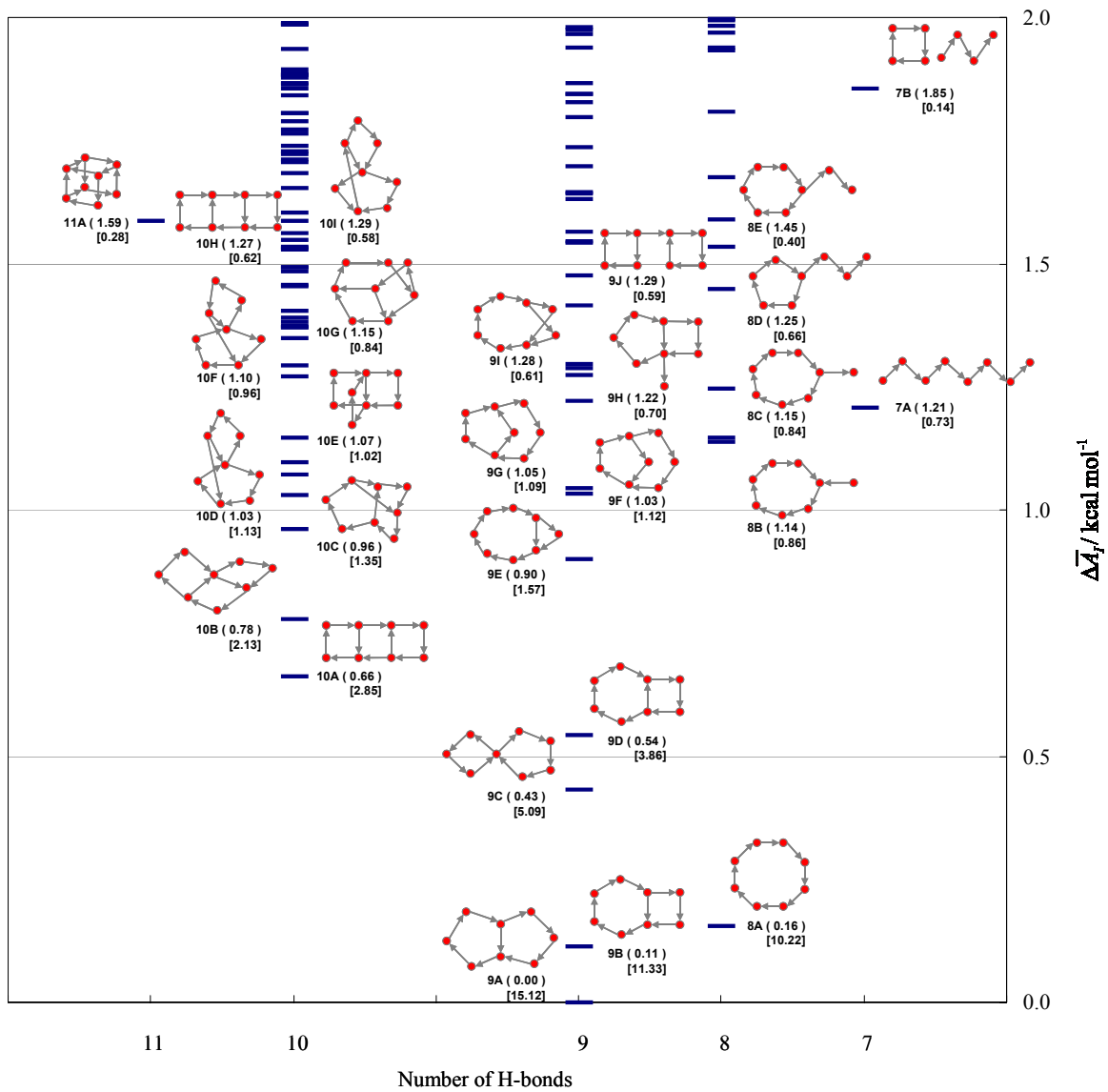
12A (D$_{2d}$)   12B (S$_4$)

Fig. 1 (Miyake & Aida)

Fig. 2 (Miyake & Aida)
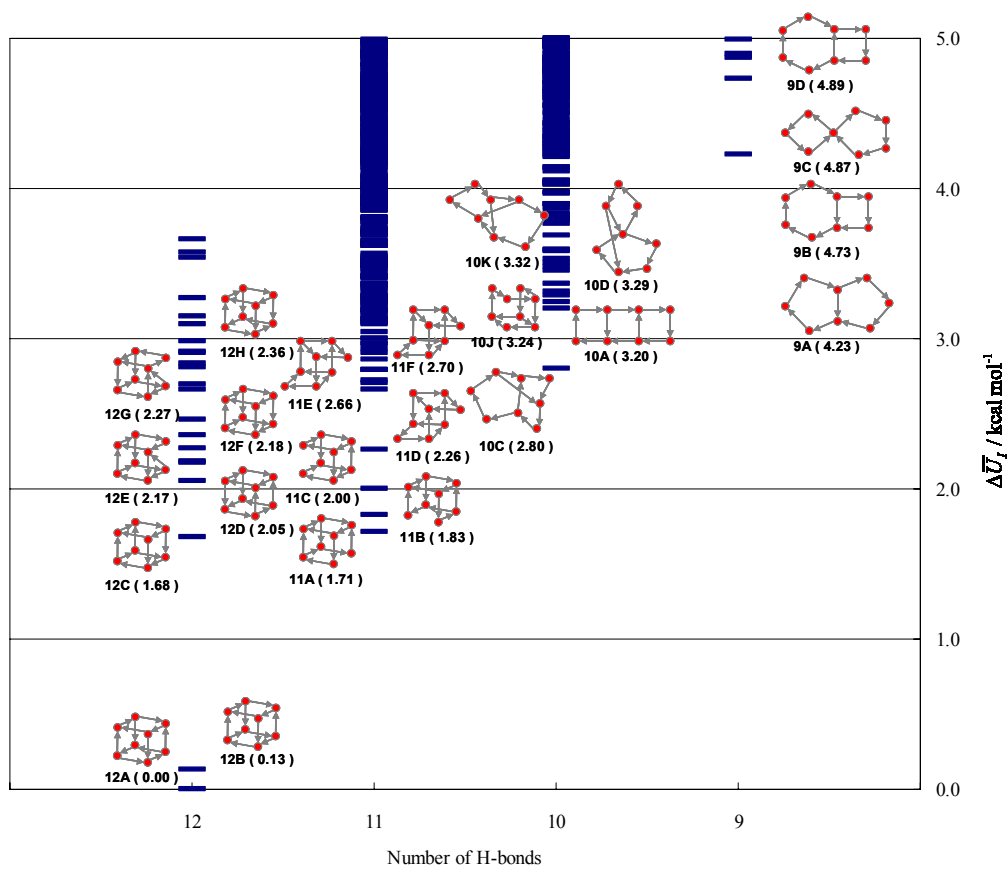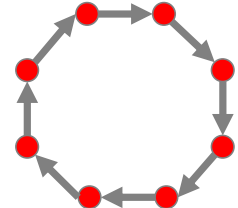
9D (4.89)

9C (4.87)

9B (4.73)

9A (4.23)

10K (3.32)

10D (3.29)

10J (3.24)

10A (3.20)

12H (2.36)

11F (2.70)

11E (2.66)

12G (2.27)

12F (2.18)

11D (2.26)

10C (2.80)

12E (2.17)

11C (2.00)

12D (2.05)

12C (1.68)

11A (1.71)

11B (1.83)

12A (0.00)

12B (0.13)

12   11   10   9

Number of H-bonds

$\Delta \overline{U}_I$ / kcal mol^{-1}
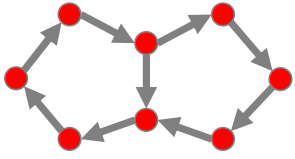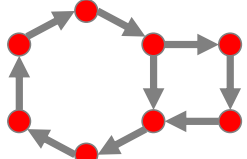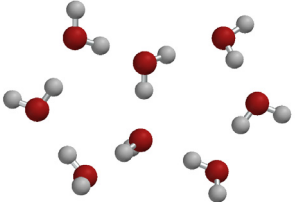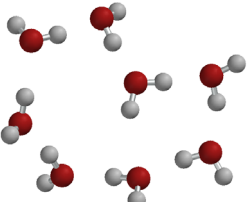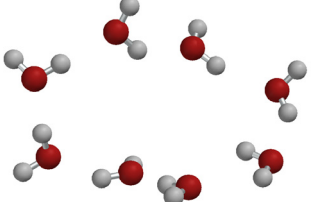
Fig. 3 (Miyake & Aida)

H-bond pattern I	9A	9B	8A
digraph			
structure			
$\Delta \overline{A}_I$ / kcal mol^{-1}	0.00	0.11	0.16
$\Delta \overline{U}_I$ / kcal mol^{-1}	0.00	0.51	1.68
$-T\Delta \overline{S}_I$ / kcal mol^{-1}	0.00	−0.39	−1.52

Fig. 4   (Miyake & Aida)

Fig. 5 (Miyake & Aida)